

## Chapter 2

# Classical fracture and failure hypotheses

In this chapter, a brief outline on classical fracture and failure hypotheses for materials under static loading will be given. The word *classical* in this context means in that most of these so-called *strength hypotheses* are already quite old. Partially they date back to considerations made at the end of the 19th or the beginning of the 20th century and they are inseparably associated with the development of solid mechanics at that time. Through modern fracture mechanics they have been pushed into the background, as far as research is regarded. However, because of their wide spreading which, last but not least, is due to their simplicity, they are still of remarkable importance.

### 2.1 Basic concepts

Strength hypotheses are intended to make a statement about the circumstances under which a material fails. Their basis are experiments conducted under specific, mostly simple, loading conditions. As an example, two typical stress-strain curves for materials under uniaxial tension are schematically shown in Fig. 2.1. Up to a

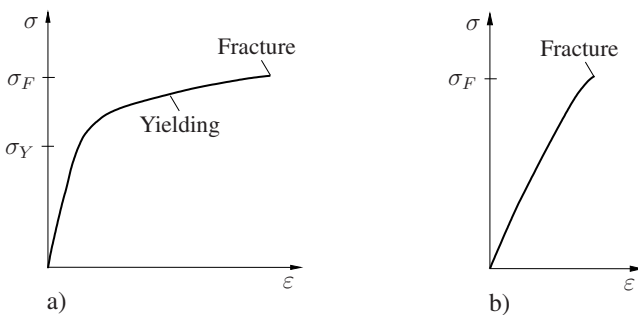


**Fig. 2.1** Material behavior: a) ductile, b) brittle

certain limit the response of many materials is essentially elastic. *Ductile* behavior is characterized through plastic deformations which occur when the stress exceeds the *yield strength*  $\sigma_Y$ . In this case, the *ultimate stress* at fracture will be attained only after sufficiently large inelastic deformations. In contrast, *brittle* material behavior is characterized by the fact that no significant inelastic deformations occur prior to fracture.

Depending on the problem at hand, the *strength* of a material is often characterized by either the yield stress or the ultimate stress at fracture. The associated material parameters are the yield strength and the ultimate tensile strength. A common feature of both is that the material behavior changes drastically at these limits. In this context it should be emphasized that ductile or brittle behavior is not a pure material property. The stress state also has an essential influence onto the material behavior. To illustrate this fact it should be mentioned that in general, a hydrostatic stress state does not lead to inelastic deformations of most materials which usually are considered as plastically deformable. Thus, under certain loading conditions, such a material can behave as absolutely brittle.

We now assume that for uniaxial loading as well as for any complex loading the actual state of the material which determines its behavior inclusive its failure limit can be characterized simply by the current stress or strain state. Then the failure condition can be expressed as

$$F(\sigma_{ij}) = 0 \quad \text{or} \quad G(\varepsilon_{ij}) = 0. \quad (2.1)$$

Just like the yield condition which is described by an analogous equation, the failure condition  $F(\sigma_{ij}) = 0$  can be interpreted as a *failure surface* in the six-dimensional stress space or alternatively in the three-dimensional space of principal stresses. Accordingly, a stress state  $\sigma_{ij}$  on the surface  $F = 0$  characterizes failure as a result of yielding or fracture.

A failure condition of the type (2.1) implies that the material state at failure is independent of the deformation history. With sufficient accuracy this applies to the onset of plastic yielding in ductile materials or to the fracture of brittle materials. Furthermore, such a failure condition is acceptable only if until failure the material can be considered as a continuum without macroscopic defects. This means in particular that macroscopic cracks must not appear and influence the behavior of the material through their presence.

The deformation process of plastically deformable materials such as metals (also concrete or geological materials often are considered as plastically deformable) after reaching the yield strength can be described by a flow rule. Such a flow rule however, by no means characterizes the kinematics of brittle fracture. In general, simple kinematic statements for fracture processes are possible only for specific stress states.

## 2.2 Failure hypotheses

Formally it is possible to establish infinitely many failure hypotheses of the type (2.1). In what follows, some common hypotheses are presented, part of which can be applied with sufficient accuracy (from an engineer's point of view) to certain classes of materials. Some of them, however, are only of historical relevance. In this context we will not again discuss the VON MISES and TRESCA yield condition since this has already been done in Section 1.3.3.1.

### 2.2.1 Principal stress hypothesis

This hypothesis dates back to W.J.M. RANKINE (1820–1872), G. LAMÉ (1795–1870), and C.L. NAVIER (1785–1836). According to this hypothesis, the material behavior is characterized by two characteristic values, the tensile strength  $\sigma_t$  and the compressive strength  $\sigma_p$ . Failure is expected to take place when the maximum principal stress reaches  $\sigma_t$  or when the minimum principal stress reaches  $-\sigma_p$ , i.e., when one of the following conditions is fulfilled:

$$\sigma_1 = \begin{cases} \sigma_t \\ -\sigma_p \end{cases} \quad \sigma_2 = \begin{cases} \sigma_t \\ -\sigma_p \end{cases} \quad \sigma_3 = \begin{cases} \sigma_t \\ -\sigma_p \end{cases} . \quad (2.2)$$

The associated failure surface in principal stress space is represented by a cube (Fig. 2.2a). The corresponding failure curve for a plane stress state ( $\sigma_3 = 0$ ) is a square (Fig. 2.2b).

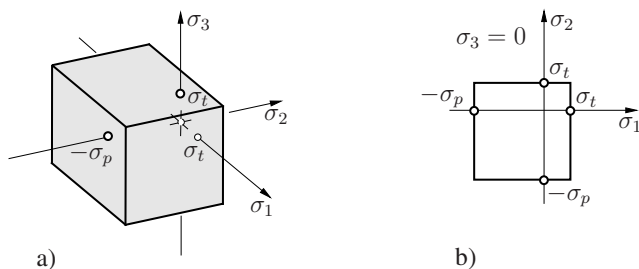


Fig. 2.2 Principal stress hypothesis

The principal stress hypothesis predominantly serves to describe brittle failure of materials. For tensile loading we generally associate with it the process of decohesion along cross sections perpendicular to the largest principal stress. The hypothesis neglects the influence of the two other principal stresses onto failure, its applicability hence is quite limited.

### 2.2.2 Principal strain hypothesis

According to the hypothesis suggested by DE SAINT-VENANT (1797–1886) and C. BACH (1889), failure occurs when the maximum principle strain reaches the critical value  $\varepsilon_t$ . If we assume linear elastic behavior until failure and introduce the critical tensile stress  $\sigma_t = E\varepsilon_t$ , we get the following failure conditions:

$$\sigma_1 - \nu(\sigma_2 + \sigma_3) = \sigma_t, \quad \sigma_2 - \nu(\sigma_3 + \sigma_1) = \sigma_t, \quad \sigma_3 - \nu(\sigma_1 + \sigma_2) = \sigma_t. \quad (2.3)$$

In this case, the failure surface is represented by a pyramid with three planes centered around the hydrostatic axis with its apex at  $\sigma_1 = \sigma_2 = \sigma_3 = \sigma_t/(1 - 2\nu)$  (Fig. 2.3a). The failure curve for plane stress is shown in Fig. 2.3b.

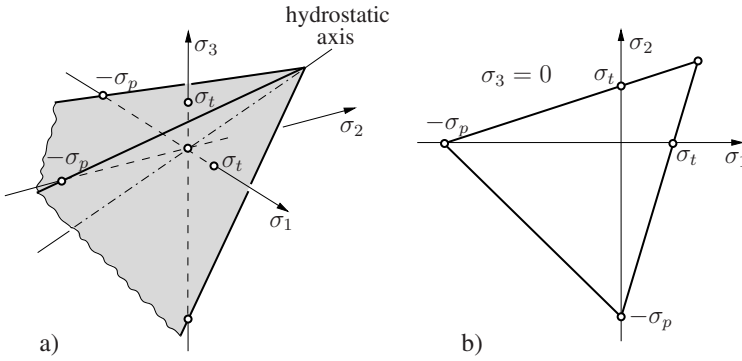


Fig. 2.3 Principal strain hypothesis

According to this hypothesis, failure under uniaxial compression should occur at  $\sigma_p = \sigma_t/\nu$ . This contradicts experimental experiences for most materials.

### 2.2.3 Strain energy hypothesis

The hypothesis by E. BELTRAMI (1835-1900) postulates failure when the strain energy density  $U$  reaches a material-specific critical value  $U_c$ , i.e., at  $U = U_c$ . Usually this assumption implies that the material behaves linearly elastic until failure. If we introduce with  $U_c = \sigma_c^2/2E$  a uniaxial failure stress  $\sigma_c$  and express  $U = U_V + U_G$  through the principal stresses by using (1.50), we obtain the following representation of the hypothesis:

$$(1+\nu)[(\sigma_1 - \sigma_2)^2 + (\sigma_2 - \sigma_3)^2 + (\sigma_3 - \sigma_1)^2] + (1-2\nu)(\sigma_1 + \sigma_2 + \sigma_3)^2 = 3\sigma_c^2. \quad (2.4)$$

The corresponding failure surface is an ellipsoid around the hydrostatic axis with the apex at  $\sigma_1 = \sigma_2 = \sigma_3 = \pm\sigma_c/\sqrt{3(1-2\nu)}$ .

According to this hypothesis, a sufficiently high hydrostatic pressure always leads to failure; this is in contradiction with experimental results. If the volumetric part  $U_V$  of the strain energy density  $U$  is omitted, Beltrami's hypothesis reduces to the von Mises yield condition.

In conjunction with modern fracture mechanics, the strain energy hypothesis in a somewhat modified form has been suggested for application as a crack initiation and propagation criterion, see S-criterion in Sect. 4.9.

### 2.2.4 Coulomb-Mohr hypothesis

This hypothesis predominantly serves to describe failure due to slip of geological and granular materials, such as sand, rock, or soils. These materials can carry only relatively small or, in the limit, no tensile stresses.

For a physical explanation we consider an arbitrary cross section which is loaded by the normal stress  $-\sigma$  (pressure) and the shear stress  $\tau$ . *Coulomb's friction law*, applied to the stresses, postulates sliding when  $\tau$  attains a critical value proportional to the pressure  $-\sigma$ :  $|\tau| = -\sigma \tan \rho$ . Here  $\rho$  is the material-dependent *friction angle*. For  $-\sigma \rightarrow 0$  it follows that  $|\tau| \rightarrow 0$ ; tensile stresses are not possible in this case. In many cases however, even for  $\sigma = 0$ , onset of sliding requires a nonzero, finite shear stress. In addition, materials frequently are able to carry tensile stresses to a certain extent. Therefore it is reasonable to modify the sliding condition as follows:

$$|\tau| = -\sigma \tan \rho + c. \quad (2.5)$$

This relation is known as the *Coulomb-Mohr hypothesis* (C.A. COULOMB (1736–1806); O. MOHR (1835–1918)). The parameter  $c$  is called *cohesion*.

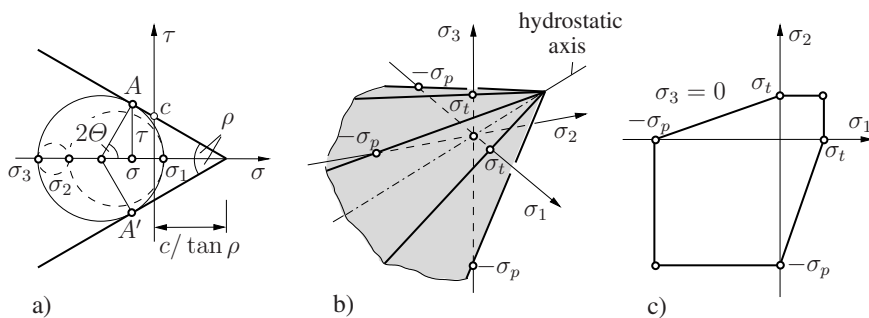


Fig. 2.4 Coulomb-Mohr hypothesis

In the  $\sigma$ - $\tau$  diagram, equation (2.5) is represented by two straight lines which form the envelop of admissible Mohr's circles (Fig. 2.4a). Sliding occurs for those stress states for which the largest of the three Mohr's circles just touches the envelope. In

terms of principal stresses this leads to the condition

$$\frac{|\sigma_1 - \sigma_3|}{2} = \left[ \frac{c}{\tan \rho} - \frac{\sigma_1 + \sigma_3}{2} \right] \sin \rho. \quad (2.6)$$

If we introduce into this equation for instance  $\sigma_1 = \sigma_t$  and  $\sigma_3 = 0$ , we obtain for the uniaxial tensile strength  $\sigma_t = 2c \cos \rho / (1 + \sin \rho)$ . Analogously, with  $\sigma_1 = 0$  and  $\sigma_3 = -\sigma_p$  the compressive strength follows to  $\sigma_p = 2c \cos \rho / (1 - \sin \rho)$ . It should also be mentioned that (2.6) includes as a special case for  $\rho \rightarrow 0$  Tresca's yield condition (cf. Sect. 1.3.3.1).

Sometimes it is appropriate to use the characteristic material parameters  $\sigma_p$  and  $\kappa = \sigma_p / \sigma_t$  instead of the parameters  $\rho$  and  $c$ . In this case it follows from (2.6) that for the onset of sliding, one of the following conditions must be fulfilled:

$$\left. \begin{array}{l} \kappa \sigma_1 - \sigma_3 \\ -\sigma_1 + \kappa \sigma_3 \end{array} \right\} = \sigma_p, \quad \left. \begin{array}{l} \kappa \sigma_2 - \sigma_1 \\ -\sigma_2 + \kappa \sigma_1 \end{array} \right\} = \sigma_p, \quad \left. \begin{array}{l} \kappa \sigma_3 - \sigma_2 \\ -\sigma_3 + \kappa \sigma_1 \end{array} \right\} = \sigma_p. \quad (2.7)$$

Here, the principal stresses are *not* a priori ordered according to their magnitude. The associated failure surface is a pyramid formed by six planes around the hydrostatic axis (Fig. 2.4b). Its apex is located at  $\sigma_1 = \sigma_2 = \sigma_3 = \sigma_p / (\kappa - 1)$ . The failure curve for a plane stress state is shown as the hexagon in Fig. 2.4c.

As already mentioned, sliding is supposed to take place in cross sections where relation (2.5) is fulfilled. They are characterized by the corresponding points  $A$  and  $A'$  in Fig. 2.4a. Accordingly, the normal of the slip plane lies in the plane given by the maximum principal stress  $\sigma_1$  and the minimum principal stress  $\sigma_3$ . The unit normal vector and the direction of  $\sigma_1$  form an angle of

$$\Theta_{1,2} = \pm(45^\circ - \rho/2). \quad (2.8)$$

According to this hypothesis, the intermediate principle stress  $\sigma_2$  has no effect on the onset of failure and the failure angle. It finally should be noted that failure along the cross section determined by relation (2.8) occurs only when it is kinematically possible.

The result (2.8) for the orientation of the failure cross section is used among others in geology to explain different types of faults of the earth's crust. Here it is

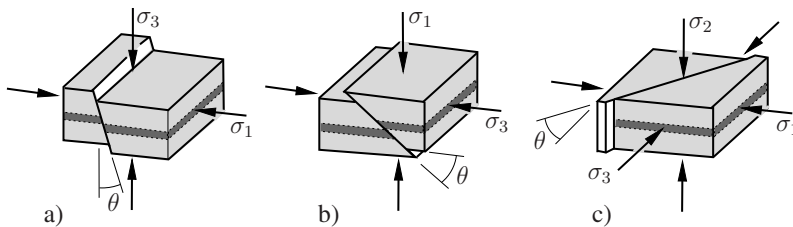


Fig. 2.5 Faults

assumed that all principal stresses are compressive stresses ( $|\sigma_3| \geq |\sigma_2| \geq |\sigma_1|$ ) and act in vertical (perpendicular to the earth's surface) and in horizontal direction, respectively. A *normal fault* then is explained with a situation where the vertical principal stress is larger than the principal stresses acting in horizontal direction (Fig. 2.5a). In contrast, for a *reverse fault* it is supposed that the value of the vertical pressure is the smallest one (Fig. 2.5b). Finally, a *strike-slip fault* is associated with a vertical pressure  $\sigma_2$  whose magnitude lies between the maximum and the minimum values of the principal stresses (Fig. 2.5c).

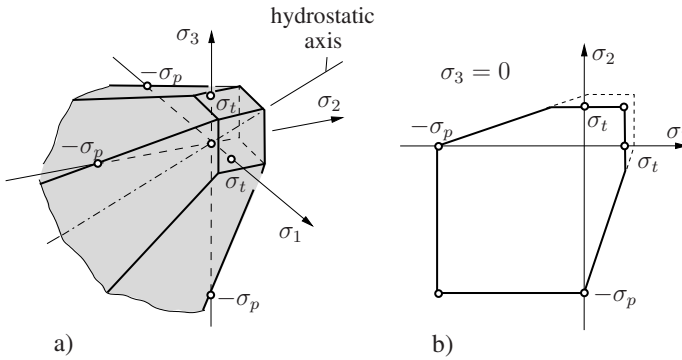


Fig. 2.6 Tension cut-off

Experiments show that the Coulomb-Mohr hypothesis describes the behavior of different materials sufficiently well in the compression regime but worse in the tension regime. Responsible for this is in most cases a change of the failure mechanism. This holds particularly when failure in the tension regime occurs not due to the sliding but is rather associated with a decohesion of the cross sections perpendicular to the maximum principal stress. A possibility to improve the failure condition consists, for instance, in a modification of the failure surface through so-called *tension cut-offs* (Fig. 2.6).

The hypothesis (2.5) assumes a linear relation between  $\tau$  and  $\sigma$ . A generalization of the form

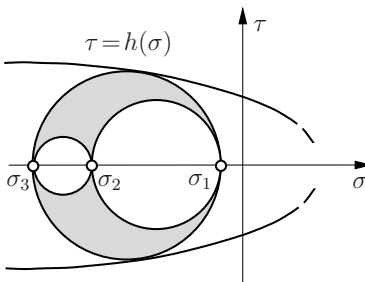


Fig. 2.7 Mohr's failure hypothesis

$$|\tau| = h(\sigma) \quad (2.9)$$

where the function  $h(\sigma)$  must be determined experimentally was proposed by O. MOHR (1900). In the  $\sigma$ - $\tau$  diagram it represents the envelope of admissible Mohr's circles (Fig. 2.7). As in hypothesis (2.5), the intermediate principal stress  $\sigma_2$  has no effect on failure. In this respect, both hypotheses may be considered as special (not general) cases of a failure condition  $F(\sigma_1, \sigma_3) = 0$ .

### 2.2.5 Drucker-Prager hypothesis

According to the hypothesis by D.C. DRUCKER (1918-2001) and W. PRAGER (1903-1980), a material fails when the condition

$$F(I_\sigma, II_s) = \alpha I_\sigma + \sqrt{II_s} - k = 0 \quad (2.10a)$$

is fulfilled. Here,  $I_\sigma$ ,  $II_s$  are the invariants of the stress tensor and of its deviator, respectively, and  $\alpha$  and  $k$  are material parameters. If we introduce  $\sigma_m = \sigma_{\text{oct}} = I_\sigma/3$  and  $\tau_{\text{oct}} = \sqrt{2 II_s/3}$  the condition (2.10a) can be interpreted similar to the Mohr-Coulomb hypothesis. Accordingly, failure occurs when the octahedral shear stress  $\tau_{\text{oct}}$  reaches a value which is linearly dependent on the normal stress  $\sigma_m$  (cf. (2.5)):

$$\tau_{\text{oct}} = -\sqrt{6} \alpha \sigma_m + \sqrt{2/3} k. \quad (2.10b)$$

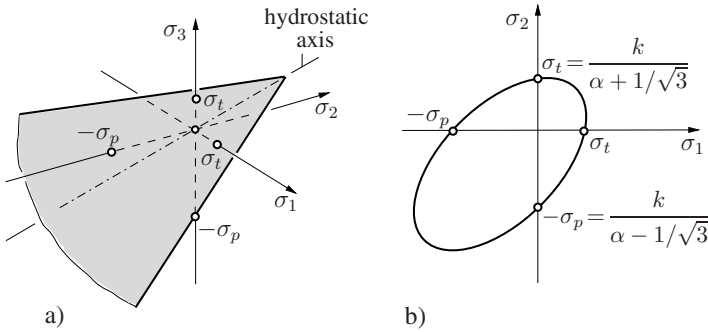


**Fig. 2.8** Drucker-Prager hypothesis

The failure surface defined by (2.10a,b) in principal stress space forms a cone around the hydrostatic axis with the apex at  $\sigma_1 = \sigma_2 = \sigma_3 = k/3\alpha$  (Fig. 2.8a). The associated failure curve for plane stress ( $\sigma_3 = 0$ ) is an ellipse (Fig. 2.8b). As the Coulomb-Mohr hypothesis, the Drucker-Prager criterion is used as a yield or as a fracture condition, predominantly for granular and geological materials. For  $\alpha = 0$  it reduces to the von Mises yield condition.



Experiments show that in some cases a description of the failure condition by means of only two material parameters is not sufficient. It then must be suitably modified. A frequently used extension of the Drucker-Prager hypothesis is given by

$$F(I_\sigma, II_s) = \alpha I_\sigma + \sqrt{II_s + \beta I_\sigma^2} - k = 0 . \quad (2.11)$$

Here,  $\beta$  is an additional material parameter.

### 2.2.6 Johnson-Cook criterion

While the failure hypotheses discussed so far are primarily intended to describe brittle failure or the onset of plastic flow, the criterion by JOHNSON and COOK (1985) addresses ductile failure after pronounced plastic deformation. Ultimate failure in many ductile materials proceeds by the formation and coalescence of microscopic voids (as discussed in more detail in Sections 3.1.3 and 9.4) which is essentially driven by hydrostatic stress. Correspondingly, the plastic strain at failure in these materials is assumed to be a decreasing function of the ratio of hydrostatic to deviatoric stress as sketched in Fig. 2.9 and approximated by the relation:

$$\varepsilon_{fail} = D_1 + D_2 \exp \left( D_3 \frac{\sigma_m}{\sigma_e} \right) . \quad (2.12)$$

Here,  $\varepsilon_{fail}$  is the value of the equivalent plastic strain  $\varepsilon_e^p = \sqrt{\frac{2}{3} \varepsilon_{ij}^p \varepsilon_{ij}^p}$  at failure,  $\sigma_m = \frac{1}{3} \sigma_{kk}$  is the hydrostatic stress,  $\sigma_e = \sqrt{\frac{3}{2} s_{ij} s_{ij}}$  the equivalent (von Mises) stress, and  $D_1, D_2, D_3$  are material constants.

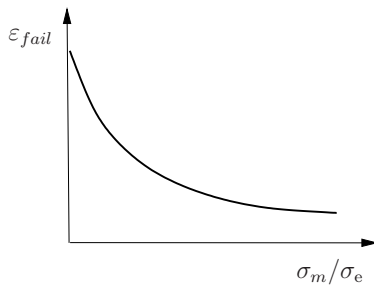


Fig. 2.9 Johnson-Cook criterion

It should be mentioned that the direct relation between the accumulated plastic strain at failure and the stress state in the failure criterion (2.12) is meaningful only if proportional loading prevails throughout the entire deformation history, i.e. when the ratio  $\sigma_m/\sigma_e$  is constant (see also Section 1.3.3.3). The model can be extended to

account for non-proportional loading by supplementing it with a damage evolution law. More elaborate models for ductile failure, however, are discussed in Sect. 9.4.

### 2.3 Deformation behavior during failure

On the basis of the failure criterion alone no direct conclusion can be drawn for the deformation behavior or the kinematics during failure. Respective statements are only possible when a specified kinematic idea is a priori associated with the failure hypothesis or when a physically meaningful assumption is introduced.

During failure due to fracture, a body is separated into two or more parts. This process is accompanied with the creation of new surfaces, i.e., with the formation of *fracture surfaces*. The associated kinematics can not be described in a simple manner. Only for sufficiently uniform stress states statements are possible which are guided by experimental results. They show two basic patterns for the formation of fracture surfaces. For a *normal stress dominated fracture*, the fracture plane coincides with the cross section normal to the maximum principal stress which necessarily must be tension (Fig. 2.10a). If the fracture surface is formed by cross sections in which a certain shear stress (e.g.,  $\tau_{\max}$ ,  $\tau_{\text{Oct}}$ , etc.) reaches a critical value, this is called *shear dominated fracture* (Fig. 2.10b). Dependent on the stress state and the material behavior, both types occur also in various mixed forms.

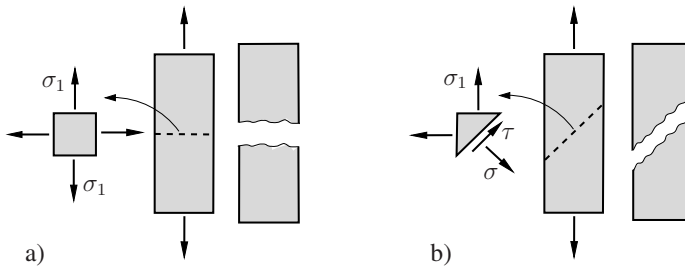


Fig. 2.10 Fracture surfaces

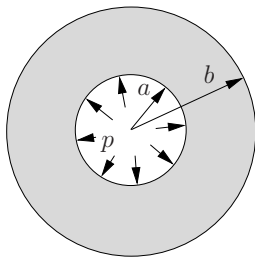
If “failure” denotes the onset of yielding, the failure criterion is equivalent to a yield criterion. Within the framework of incremental plasticity, deformations appearing during yielding can be described by means of the flow rule  $d\varepsilon_{ij}^p = d\lambda \partial F / \partial \sigma_{ij}$  (cf. Sect. 1.3.3.2). The respective equations for the von Mises and Tresca yield conditions are assembled in (1.83a) and (1.84). As a further example, the incremental stress-strain relations for the Drucker-Prager model shall be specified here. We assume that the yield surface is independent of the deformation history (perfectly plastic material). In this case, the flow rule in conjunction with (2.10a,b) and  $I_\sigma = \sigma_{kk} = \sigma_{ij}\delta_{ij}$  and  $\Pi_s = \frac{1}{2}s_{ij}s_{ij}$  yields

$$d\varepsilon_{ij}^p = d\lambda \left( \alpha \delta_{ij} + \frac{s_{ij}}{2\sqrt{H_s}} \right). \quad (2.13)$$

The determination of  $d\lambda$  is not further discussed here. It should be noted that according to (2.12) volume changes generally occur; the corresponding increment is given by  $d\varepsilon_{kk}^p = 3\alpha d\lambda$ . However, experiments suggest that the associated flow rule is not valid for granular materials. Thus, yielding then takes place not perpendicular to the yield surface. Therefore, equation (2.13) should not be used for such materials.

## 2.4 Problems

**Problem 2.1** a) Determine the stress distribution in a linear elastic thick-walled cylinder (radii  $a$  and  $b$ ) subjected to an internal pressure  $p$  by using the complex potentials



$$\Phi(z) = Az, \quad \Psi(z) = \frac{B}{z}.$$

b) Find the potential failure loci according to the maximum principal stress criterion and the maximum shear stress criterion.

Fig. 2.11

### Solution

a)

$$\sigma_\varphi = p \frac{(b/r)^2 + 1}{(b/a)^2 - 1} = \sigma_1 > 0, \quad \sigma_r = p \frac{(b/r)^2 - 1}{(b/a)^2 - 1} = \sigma_2 < 0, \quad \tau_{r\varphi} = 0.$$

b) Maximum principal stress criterion: Since  $\sigma_\varphi = \sigma_1$  is the maximum principal stress, failure should occur perpendicular to the hoop stress, i.e. in radial sections.

Maximum shear stress criterion: On account of  $\tau_{r\varphi} = 0$ , the maximum shear direction is everywhere inclined by  $45^\circ$  with respect to the radial direction. This can be expressed by the differential relation  $dr = r d\varphi$  which has the solution  $\varphi(r) = \varphi_0 + \ln(r/a)$ ; i.e. failure takes place along logarithmic spirals.

## 2.5 Further reading

Gould, P.L. *Introduction to Linear Elasticity*. Springer, New York, 1993

Paul, B. *Macroscopic Criteria for Plastic Flow and Brittle Fracture*. In *Fracture – A Treatise*, Vol. 2, ed. H. Liebowitz, pp. 315-496, Academic Press, London, 1968

Nadai, A. *Theory of Flow and Fracture of Solids*, Vol. 1. McGraw-Hill, New York, 1963

Fracture Mechanics

With an Introduction to Micromechanics

Gross, D.; Seelig, Th.

2011, X, 336 p., Hardcover

ISBN: 978-3-642-19239-5